SIMULTANEOUS STABILIZATION OF POWER SYSTEMS EQUIPPED WITH UNIFIED POWER FLOW CONTROLLER USING PARTICLE SWARM

Ali T. Al-Awami
King Fahd University of Petroleum & Minerals, Dhahran, Saudi Arabia
aliawami@kfupm.edu.sa

Y. L. Abdel-Magid
King Fahd University of Petroleum & Minerals, Dhahran, Saudi Arabia
amagid@kfupm.edu.sa

M. A. Abido
King Fahd University of Petroleum & Minerals, Dhahran, Saudi Arabia
mabido@kfupm.edu.sa

Abstract – In this paper, the use of the supplementary controller of a unified power flow controller (UPFC) to damp low frequency oscillations in a weakly connected system is investigated. The potential of the UPFC supplementary controllers to enhance the dynamic stability is evaluated by measuring the electromechanical (EM) controllability through singular value decomposition (SVD) analysis. Individual designs of UPFC controllers using particle swarm optimization (PSO) technique are discussed. To ensure the robustness of the proposed stabilizers, the design process takes into account a wide range of operating conditions. The effectiveness of the proposed controllers in damping low frequency oscillations is verified through eigenvalue analysis and non-linear time simulation. A comparison with a robust power system stabilizer is also included.

Keywords: UPFC, power system stability, PSO, SVD, simultaneous stabilization

1 INTRODUCTION

As power demand grows rapidly and expansion in transmission and generation is restricted, power systems are today much more loaded than before. This causes the power systems to be operated near their stability limits. In addition, interconnection between remotely located power systems gives rise to low frequency oscillations in the range of 0.1-3.0 Hz. If not well damped, these oscillations may keep growing in magnitude until loss of synchronism results.

Power system stabilizers (PSSs) have been used in the last few decades to serve the purpose of enhancing power system damping to low frequency oscillations. PSSs have proved to be efficient in performing their assigned tasks. However, they may adversely affect voltage profile and may not be able to suppress oscillations resulting from severe disturbances, especially those which may occur at the generator terminals.

A wide spectrum of PSS tuning approaches has been proposed. These approaches have included pole placement [1], damping torque concepts [2], H_∞ [3], and variable structure [4], and the different optimization and artificial intelligence techniques [5,6].

FACTS devices have shown very promising results when used to improve power system steady-state performance. Because of the extremely fast control action associated with FACTS-device operations, they have been very promising candidates for utilization in power system damping enhancement.

A unified power flow controller (UPFC) is the most promising device in the FACTS concept. It has the ability to adjust the three control parameters, i.e. the bus voltage, transmission line reactance, and phase angle between two buses, either simultaneously or independently. A UPFC performs this through the control of the in-phase voltage, quadrature voltage, and shunt compensation. Till now, not much research has been devoted to the analysis and control of UPFCs.

Several trials have been reported in the literature to model a UPFC for steady-state and transient studies. Based on Nabavi-Iravani model [7], Wang developed a linearized UPFC model [8] which has been incorporated into the Heffron-Phillips model.[9]

A number of control schemes have been suggested to perform the oscillation-damping task. Huang et al. [10] attempted to design a conventional fixed-parameter lead-lag controller for a UPFC installed in the tie line of a two-area system to damp the interarea mode of oscillation. Mok et al. [11] considered the design of an adaptive fuzzy logic controller for the same purpose. Dash et al. [12] suggested the use of a radial basis function NN for a UPFC to enhance system damping performance. Robust control schemes, such as H_∞ and singular value analysis, have also been explored [13,14]. To avoid pole-zero cancellation associated with the H_∞ approach, the structured singular value analysis have been utilized in [15] to select the parameters of the UPFC controller to have the robust stability against model uncertainties.

In this paper, singular value decomposition (SVD) is used to select the UPFC control signals which are most suitable for damping the electromechanical (EM) mode oscillations. A SMIB system equipped with a UPFC controller is used in this study. The problem of damping controllers design is formulated as an optimization problem to be solved using PSO. The aim of the optimization is to search for the optimum controller parameter settings that maximize the minimum damping ratio of the system complex modes. To ensure the robustness of the proposed stabilizers, the design process takes into account several loading conditions. Damping torque coefficient, eigenvalue and non-linear simulation analyses are used to assess the effectiveness of the proposed stabilizers to damp low frequency oscillations. A comparison with a robust power system stabilizer is also included.

2 PROBLEM STATEMENT

Figure 1 shows a SMIB system equipped with a UPFC. The UPFC consists of an excitation transformer (ET), a boosting transformer (BT), two three-phase GTO based voltage source converters (VSCs), and a DC link capacitors. The four input control signals to the UPFC are m_E, m_B, δ_E, *and* δ_B, where

m_E is the excitation amplitude modulation ratio,
m_B is the boosting amplitude modulation ratio,
δ_E is the excitation phase angle, and
δ_B is the boosting phase angle.

2.1 Power System Model

By applying Park's transformation and neglecting the resistance and transients of the ET and BT transformers, the UPFC can be modeled as [7,8]:

$$\begin{bmatrix} v_{Etd} \\ v_{Etq} \end{bmatrix} = \begin{bmatrix} 0 & -x_E \\ x_E & 0 \end{bmatrix} \begin{bmatrix} i_{Ed} \\ i_{Eq} \end{bmatrix} + \begin{bmatrix} \frac{m_E \cos\delta_E v_{dc}}{2} \\ \frac{m_E \sin\delta_E v_{dc}}{2} \end{bmatrix} \quad (1)$$

$$\begin{bmatrix} v_{Btd} \\ v_{Btq} \end{bmatrix} = \begin{bmatrix} 0 & -x_B \\ x_B & 0 \end{bmatrix} \begin{bmatrix} i_{Bd} \\ i_{Bq} \end{bmatrix} + \begin{bmatrix} \frac{m_B \cos\delta_B v_{dc}}{2} \\ \frac{m_B \sin\delta_B v_{dc}}{2} \end{bmatrix} \quad (2)$$

$$\dot{v}_{dc} = \frac{3m_E}{4C_{dc}} \begin{bmatrix} \cos\delta_E & \sin\delta_E \end{bmatrix} \begin{bmatrix} i_{Ed} \\ i_{Eq} \end{bmatrix} + \frac{3m_B}{4C_{dc}} \begin{bmatrix} \cos\delta_B & \sin\delta_B \end{bmatrix} \begin{bmatrix} i_{Bd} \\ i_{Bq} \end{bmatrix} \quad (3)$$

where v_{Et}, i_E, v_{Bt}, and i_B are the excitation voltage, excitation current, boosting voltage, and boosting current, respectively; C_{dc} and v_{dc} are the DC link capacitance and voltage, respectively.

The non-linear model of the SMIB system of Figure 1 is:

$$\dot{\delta} = \omega_b(\omega - 1) \quad (4)$$

$$\dot{\omega} = (P_m - P_e - D(\omega - 1))/M \quad (5)$$

$$\dot{E}_q^{'} = (E_{fd} - (x_d - x_d^{'})i_d - E_q^{'})/T_{do}^{'} \quad (6)$$

$$\dot{E}_{fd} = (K_A(V_{ref} - v + u_{PSS}) - E_{fd})/T_A \quad (7)$$

where

$$P_e = v_d i_d + v_q i_q, v = (v_d^2 + v_q^2)^{1/2}, v_d = x_q i_q,$$
$$v_q = E_q^{'} - x_d^{'} i_d, i_d = i_{Ed} + i_{Bd}, i_q = i_{Eq} + i_{Bq}$$

P_m and P_e are the input and output power, respectively; M and D the inertia constant and damping coefficient, respectively; ω_b the synchronous speed; δ and ω the rotor angle and speed, respectively; $E_q^{'}$, E_{fd}, and v the generator internal, field and terminal voltages, respectively; $T_{do}^{'}$ the open circuit field time constant; x_d, $x_d^{'}$, and x_q the d-axis reactance, d-axis transient reactance, and q-axis reactance, respectively; K_A and T_A the exciter gain and time constant, respectively; V_{ref} the reference voltage; and u_{PSS} the PSS control signal.

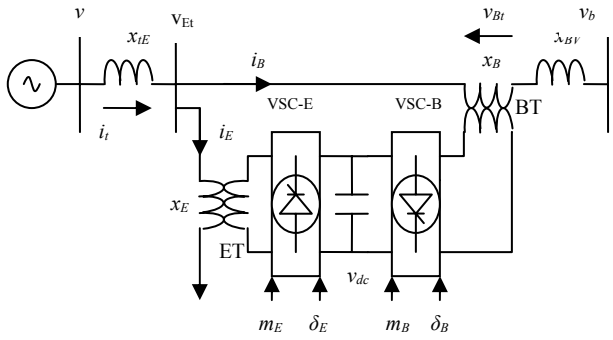

Figure 1: SMIB power system equipped with UPFC

The non-linear dynamic equations can be linearized around a given operating point to have the linear model given below:

$$\dot{x} = Ax + Bu \quad (8)$$

where

$$x = \begin{bmatrix} \Delta\delta & \Delta\omega & \Delta E_q' & \Delta E_{fd} & \Delta v_{dc} \end{bmatrix}^T$$
$$u = \begin{bmatrix} \Delta u_{pss} & \Delta m_E & \Delta\delta_E & \Delta m_b & \Delta\delta_b \end{bmatrix}^T$$

$$A = \begin{bmatrix} 0 & \omega_b & 0 & 0 & 0 \\ -\frac{K_1}{M} & -\frac{D}{M} & -\frac{K_2}{M} & 0 & -\frac{K_{pd}}{M} \\ -\frac{K_4}{T_{do}'} & 0 & -\frac{K_3}{T_{do}'} & \frac{1}{T_{do}'} & -\frac{K_{qd}}{T_{do}'} \\ -\frac{K_A K_5}{T_A} & 0 & -\frac{K_A K_6}{T_A} & -\frac{1}{T_A} & -\frac{K_A K_{vd}}{T_A} \\ K_7 & 0 & K_8 & 0 & -K_9 \end{bmatrix}$$

$$B = \begin{bmatrix} 0 & 0 & 0 & 0 & 0 \\ 0 & -\frac{K_{pe}}{M} & -\frac{K_{p\delta e}}{M} & -\frac{K_{pb}}{M} & -\frac{K_{p\delta b}}{M} \\ 0 & -\frac{K_{qe}}{T_{do}'} & -\frac{K_{q\delta e}}{T_{do}'} & -\frac{K_{qb}}{T_{do}'} & -\frac{K_{q\delta b}}{T_{do}'} \\ \frac{K_A}{T_A} & -\frac{K_A K_{ve}}{T_A} & -\frac{K_A K_{v\delta e}}{T_A} & -\frac{K_A K_{vb}}{T_A} & -\frac{K_A K_{v\delta b}}{T_A} \\ 0 & K_{ce} & K_{c\delta e} & K_{cb} & K_{c\delta b} \end{bmatrix}$$

$K_1 - K_9$, K_{pu}, K_{qu}, and K_{vu} are linearization constants.

2.2 PSS and UPFC Controllers

The PSS structure to be considered is the very widely used lead-lag controller, whose transfer function is

$$u_{pss} = K \frac{sT_w}{1 + sT_w} \left(\frac{1 + sT_1}{1 + sT_2} \right) \left(\frac{1 + sT_3}{1 + sT_4} \right) \Delta\omega \quad (9)$$

The UPFC damping controllers are of the structure shown in Figure 2, where u can be m_E, δ_E, m_B, or δ_B.

In order to maintain the power balance between the series and shunt converters, a DC voltage regulator must be incorporated. The DC voltage is controlled through modulating the phase angle of the ET voltage, δ_E. Therefore, the δ_E damping controller to be considered is

that shown in Figure 3, where the DC voltage regulator is a PI-controller.

2.3 Objective Function and Stabilizer Design

In this study, several loading conditions, including nominal, light, heavy, and leading power factor without and with system parameter uncertainties, are considered to ensure the robustness of the proposed stabilizers. To select the best stabilizer parameters that most enhance the power system transient performance, the problem is formulated so as to optimize a selected objective function J subject to some inequality constraints, which are the maximum and minimum limits of each controller gain K and time constants T_1- T_4.

In this work,

$$J=min\{\zeta_i\} \quad (10)$$

where $min\{\zeta_i\}$ is the damping ratio corresponding to the least damped complex mode of the ith loading condition.

That is, for loading condition i, λ_i is a vector of the eigenvalues of system matrix A_i. And, ζ_i is a vector of the corresponding damping ratios of λ_i, where

$$\zeta_i = cos\{\pi - tan^{-1}[Im(\lambda_i) / Re(\lambda_i)]\}$$

Hence, the design problem can be formulated as:

maximize J

Subject to

$$K^{\min} \le K \le K^{\max}$$

$$T_1^{\min} \le T_1 \le T_1^{\max}$$

$$T_2^{\min} \le T_2 \le T_2^{\max}$$

$$T_3^{\min} \le T_3 \le T_3^{\max}$$

$$T_4^{\min} \le T_4 \le T_4^{\max}$$

The proposed approach employs PSO to search for the optimum parameter settings of the given controllers.

3 CONTROLLABILITY MEASURE

To measure the controllability of the EM mode by a given input (control signal), the singular value decomposition (SVD) is employed. Mathematically, if G is an $m \times n$ complex matrix, then there exist unitary matrices W and V with dimensions of $m \times m$ and $n \times n$, respectively, such that

$$G = W\Sigma V \quad (11)$$

where

$$\Sigma = \begin{bmatrix} \Sigma_1 & 0 \\ 0 & 0 \end{bmatrix}, \ \Sigma_1 = diag(\sigma_1, \ldots, \sigma_r) \quad (12)$$

with $\sigma_1 \ge \ldots \ge \sigma_r \ge 0$ where $r=min\{m,n\}$
and $\sigma_1, \ldots, \sigma_r$ are the singular values of G.

The minimum singular value σ_r represents the distance of the matrix G from all the matrices with a rank of r-1. This property can be used to quantify modal controllability based on matrices A and B of equation (8) [16,17]. The matrix B can be written as $B=[b_1\ b_2\ b_3\ b_4\ b_5]$ where b_i is a column vector corresponding to the ith input. The minimum singular value, σ_{min}, of the matrix $[\lambda I-A\ b_i]$ indicates the capability of the ith input to control the mode associated with the eigenvalue λ.

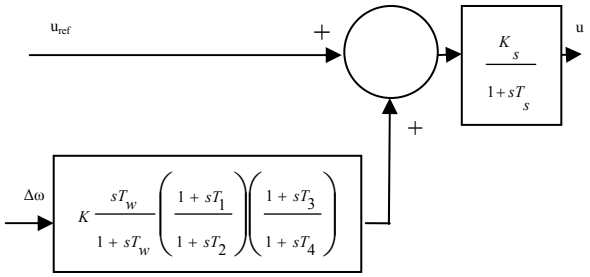

Figure 2: UPFC with lead-lag controller

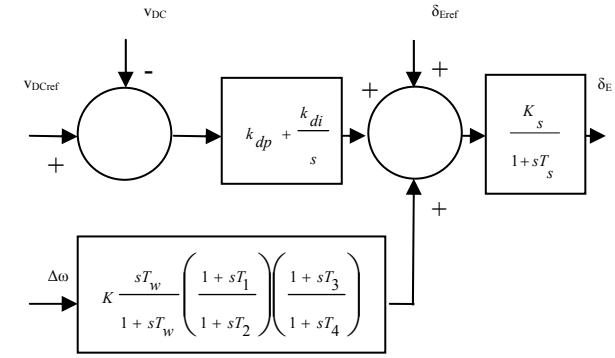

Figure 3: UPFC with lead-lag controller and DC voltage regulator

Actually, the higher the σ_{min}, the higher the controllability of this mode by the input considered. As such, the controllability of the EM mode can be examined with all inputs in order to identify the most effective one to control the mode.

4 PARTICLE SWARM OPTIMIZER

A novel population based optimization approach, called Particle Swarm Optimization (PSO) approach, was introduced first in [18]. This new approach features many advantages; it is simple, fast and can be coded in few lines. Also, its storage requirement is minimal. Another advantage of PSO is that the initial population of the PSO is maintained, and so there is no need for applying operators to the population, a process that is time- and memory-storage-consuming. [18,19]

PSO starts with a population of random solutions "particles" in a D-dimension space. The ith particle is represented by $X_i=(x_{i1}, x_{i2}, \ldots, x_{iD})$. Each particle keeps track of its coordinates in hyperspace, which are associated with the fittest solution it has achieved so far. The value of the fitness for particle i (*pbest*) is also stored as $P_i=(p_{i1}, p_{i2}, \ldots, p_{iD})$. The global version of the PSO keeps track of the overall best value (*gbest*), and its location, obtained thus far by any particle in the population [18,19].

PSO consists of, at each step, changing the velocity of each particle toward its pbest and gbest according to equation (13). The velocity of particle i is represented as $V_i=(v_{i1}, v_{i2}, \ldots, v_{iD})$. Acceleration is weighted by a

random term, with separate random numbers being generated for acceleration toward pbest and gbest. The position of the *i*th particle is then updated according to equation (14) [18,19].

$$v_{id} = w*v_{id} + c_1*rand( )*(p_{id}-x_{id}) + c_2*Rand( )*(p_{gd}-x_{id}) \quad (13)$$

$$x_{id} = x_{id} + v_{id} \quad (14)$$

where, $p_{id} = pbest$ and $p_{gd} = gbest$

The PSO Algorithm can be described as follows:

Step1: Initialize an array of particles with random positions and their associated velocities to satisfy the inequality constraints.

Step 2: Check for the satisfaction of the equality constraints and modify the solution if required.

Step 3: Evaluate the fitness function of each particle.

Step 4: Compare the current value of the fitness function with the particles' previous best value (*pbest*). If the current fitness value is less, then assign the current fitness value to *pbest* and assign the current coordinates (positions) to *pbestx.*

Step 5: Determine the current global minimum fitness value among the current positions.

Step 6: Compare the current global minimum with the previous global minimum (*gbest*). If the current global minimum is better than gbest, then assign the current global minimum to *gbest* and assign the current coordinates (positions) to *gbestx.*

Step 7: Change the velocities according to equation (13), move each particle to the new position according to equation (14) and return to Step 2.

Step 8: Repeat Step 2- Step 7 until a stopping criterion is satisfied.

5 SIMULATION RESULTS

5.1 Controllability Measure

SVD is employed to measure the controllability of the EM mode from each of the five inputs: u_{pss}, m_E, δ_E, m_B, and δ_B. The minimum singular value, σ_{min}, is estimated over a wide range of operating conditions. For SVD analysis, P_e ranges from 0.05 to 1.4 pu and Q_e= [-0.4, 0, 0.4]. At each loading condition, the system model is linearized, the EM mode is identified, and the SVD-based controllability measure is implemented.

For comparison purposes, the minimum singular value for all inputs at Q_e= 0.4 pu is shown in Figure 4. From this figure, the following can be noticed:

- EM mode controllability via δ_E is not affected much by loading conditions.
- The EM mode is more controllable with δ_E, m_B, and PSS than with either m_E or δ_B.
- All control signals except δ_E suffer from low controllability to EM mode at low loading conditions.

5.2 Stabilizer Design

The objective is to design robust stabilizers to ensure their effectiveness over a wide range of operating conditions. The design process takes into account several loading conditions including nominal, light, heavy, and leading power factor conditions. These conditions are considered without and with system parameter uncertainties, such as machine inertia, line impedance, and field time constant. The total number of 16 operating conditions is considered during the design process as given in Table 1

PSO is used to optimize the parameters of each controller that maximizes the minimum damping ratio of all the complex eigenvalues associated with the 16 operating points simultaneously. The final settings of the optimized parameters for the proposed stabilizers are given in Table 2. It is worth mentioning that the optimization of the m_E- and δ_B-based stabilizers parameter settings gives rise to unstable EM modes. That is, these two stabilizers cannot simultaneously stabilize the EM mode for all the 16 operating conditions. Hence, these stabilizers and their results are excluded from the analysis hereafter.

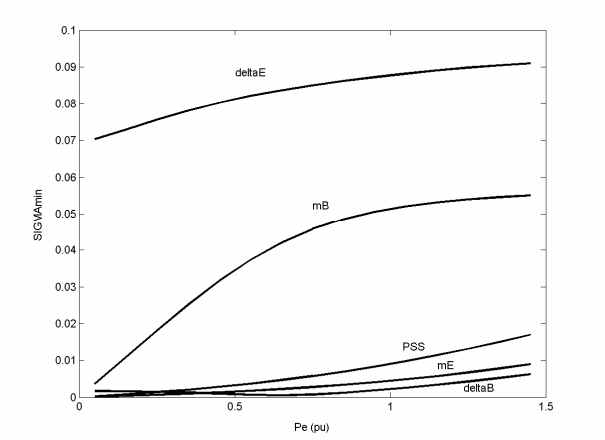

Figure 4: Minimum singular value with all stabilizers at Q_e=0.4

Loading Condition (P_e, Q_e) pu	Parameter Uncertainties
Nominal (1.0, 0.015)	No parameter uncertainties
Light (0.3, 0.100)	30% increase of line reactance X_{BV}
Heavy (1.1, 0.100)	25% decrease of machine inertia M
Leading Pf (0.7, -0.30)	30% decrease of field time constant T'_{do}

Table 1: Loading conditions and parameter uncertainties considered in the design stage

	δ_E	m_B	PSS
K	100.00	19.017	42.262
$\mathbf{T_1}$	0.0868	5.0000	0.1093
$\mathbf{T_2}$	1.2140	0.8077	1.4177
$\mathbf{T_3}$	5.0000	0.1458	2.6284
$\mathbf{T_4}$	1.1200	0.0100	0.0100
ζ	0.4545	0.3900	0.2800

Table 2: The optimal parameter settings of the individual controllers

	No parameter uncertainties	30% increase of line reactance X	25% decrease of machine inertia M	30% decrease of field time constant T'_{do}
Nominal	1.5033±5.3328i, **-0.2713**	1.4191±4.9900i, **-0.2735**	1.8047±5.9408i, **-0.2907**	1.5034±5.4025i, **-0.2681**
Light	1.3952±5.0825i, **-0.2647**	1.3254±4.7414i, **-0.2692**	1.6730±5.6676i, **-0.2831**	1.3951±5.0913i, **-0.2643**
Heavy	1.4138±5.0066i, **-0.2718**	1.2553±4.5295i, **-0.2671**	1.7027±5.5775i, **-0.2920**	1.4038±5.0846i, **-0.2661**
Leading Pf	1.4502±5.3584i, **-0.2612**	1.4092±5.0888i, **-0.2669**	1.7461±5.9774i, **-0.2804**	1.4498±5.3952i, **-0.2595**

Table 3: Open-loop eigenvalues and corresponding damping ratios **(bold)** associated with the EM modes of all the 16 points considered in the robust design process

	δ_E	m_B	PSS
Nominal	-6.5930 ±10.068i, **0.6027**	-2.0800 ± 2.8100i, **0.5900**	-5.4300 ± 0.9900i, **0.9800**
Light	-2.2726 ± 2.7631i, **0.6352**	-2.0300 ± 2.5400i, **0.6200**	-1.4900 ± 5.0500i, **0.2800**
Heavy	-1.2901 ± 1.9892i, **0.5441**	-1.5600 ± 1.8600i, **0.6400**	-2.0900 ± 1.6600i, **0.7800**
Leading Pf	-2.0346 ± 3.9874i, **0.4545**	-1.7400 ± 4.0600i, **0.3900**	-5.8600 ± 2.9600i, **0.8900**

Table 4: System eigenvalues and corresponding damping ratios at all loading conditions

For reference, Table 3 lists the open-loop eigenvalues and corresponding damping ratios associated with the EM modes of all the 16 operating points considered in the robust design process. It is evident that all these modes are unstable.

It is worth mentioning that k_{dp} and k_{di}, the DC voltage regulator gains shown in Figure 3, have been set a priori to the values shown in the Appendix.

5.3 Damping Torque Coefficient

To evaluate the effectiveness of the proposed stabilizers, the damping torque coefficient (K_d) has been estimated with PSS, m_B- and δ_E-based stabilizers when designed individually. Figure 5 shows K_d versus the loading variations with the three stabilizers. From the figure, the following can be noticed:

- Damping torque coefficient via δ_E is almost unaffected by loading levels.
- The PSS is the most effective stabilizer at nominal and high loading. However, δ_E becomes the winner at light loading.
- The m_B, and PSS suffer from negative damping characteristics at light loading.

5.4 Eigenvalue Analysis and Time-Domain Simulations

The system EM modes and their corresponding damping ratios with the proposed PSS, m_B- and δ_E-based stabilizers when applied at the four loading conditions, nominal, light, heavy, and leading power factor, are given in Table 4. It is evident that, using the proposed stabilizers design, the damping ratio of the EM mode eigenvalue is greatly enhanced.

Moreover, the nonlinear time-domain simulations are carried out at the nominal, light, and leading power factor loading conditions specified previously. The speed deviations for a 6-cycle three-phase fault at nominal and light loading and for a 3-cycle fault at leading power factor loading condition are shown in Figures 6, 7 and 8 respectively.

From these results, it can be concluded that:

- m_B- and δ_E-based stabilizers provide the least overshoot during the first swing.
- The performance of δ_E-based stabilizer is almost unaffected with loading conditions. This ensures the robustness of this stabilizer.
- At light loading, δ_E-based stabilizer is the most effective in damping low frequency oscillations. The performance of m_B-based stabilizer and PSS, however, is degraded at this loading condition.

Generally, these results confirm those conclusions drawn from damping torque analysis and eigenvalue analysis results.

6 CONCLUSION

In this paper, SVD has been employed to evaluate the EM mode controllability to the four UPFC control signals. It has been shown that the EM mode is most strongly controlled via δ_E for a wide range of loading conditions. In addition, SVD analysis has illustrated that the EM mode is poorly controlled through m_E and δ_B.

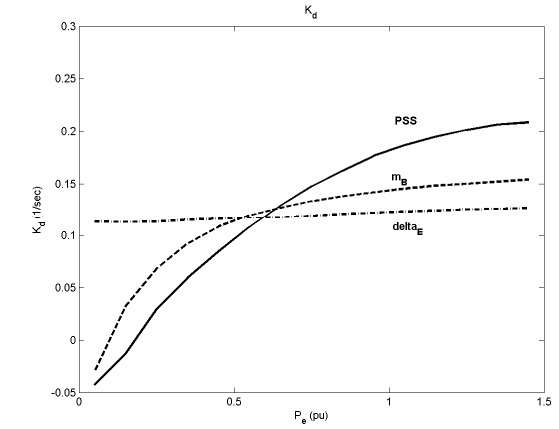

Figure 5: Damping torque coefficient with load variations, Q=0.4 pu.

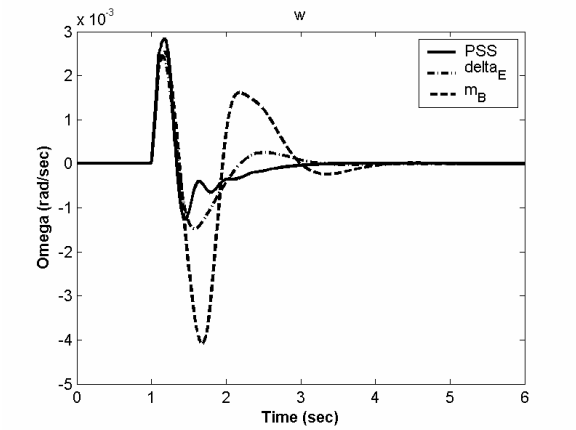

Figure 6: System response to 6-cycle fault disturbance at nominal loading

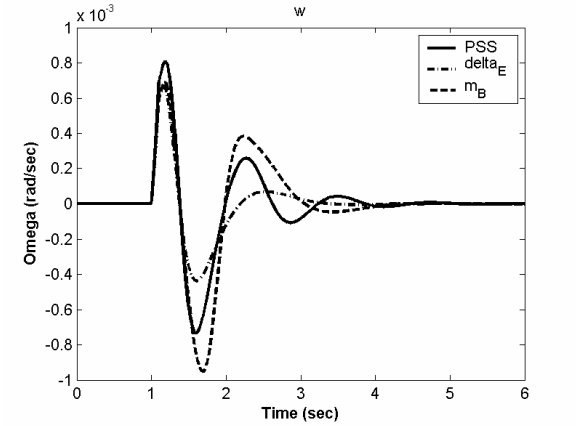

Figure 7: System response to 6-cycle fault disturbance at light loading

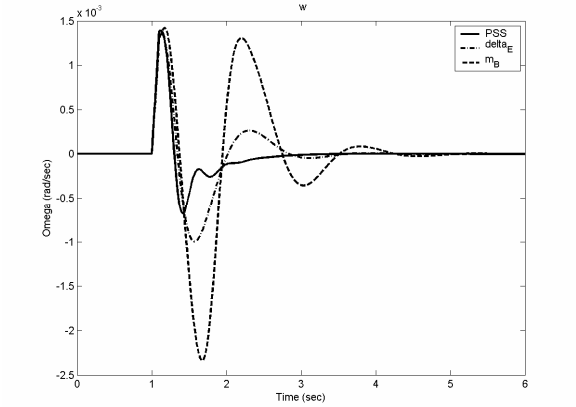

Figure 8: System response to 3-cycle fault disturbance at leading power factor loading

An optimization technique has been proposed to design the UPFC controllers individually. PSO has been utilized to search for the optimal controller parameter settings that optimize an eigenvalue-based objective function. To guarantee the robustness of the proposed controllers, the design process is carried out considering a wide range of operating conditions. PSS is included for comparison purposes. Simulation results through nonlinear power system model have proved the conclusions drawn from SVD analysis.

7 ACKNOWLEDGMENTS

The authors would like to acknowledge King Fahd University of Petroleum and Minerals for the support of this work.

8 APPENDIX

The test system parameters are:
Machine: x_d=1; x_q=0.6; x'_d=0.3; D=0; M=8.0; T'_{do}=5.044; $freq$=60; v=1.05;
Exciter : K_A=50; T_A=0.05; E_{fd_max}=7.3; E_{fd_min}=-7.3;
PSS: T_w=5; T_{i_min}=0.05; T_{i_max}=1.5; i=1,2,3,4; $upss_{\_max}$=0.2; u_{pss_min}=-0.2;
DC voltage regulator: k_{dp}=-10; k_{di}=0;
Transmission Line: x_{tE}=0.1; x_{BV}=0.6;
UPFC: x_E=0.1; x_B=0.1; K_s=1; T_s=0.05; C_{dc}=3; V_{dc}=2; m_{B_max}=2; m_{B_min}=0.

REFERENCES

[1] C. L. Chen and Y. Y. Hsu, "Coordinated synthesis of multimachine power system stabilizer using an efficient decentralized modal control (DMC) algorithm," IEEE Trans. on Power Systems, Vol. 9, no. 3 , 1987, pp. 543-551

[2] M. J. Gibbard, "Co-ordinated design of multimachine power system stabilisers based on damping torque concepts," IEE Proc. Pt. C, Vol. 135, No. 4, 1988, pp. 276-284.

[3] M. Klein, L.X. Le, G.J. Rogers, S. Farrokhpay, and N.J. Balu, "H_∞ damping controller design in large power systems**,"** IEEE Trans. on Power Systems, Vol. 10, no. 1 , Feb. 1995, pp. 158 -166

[4] V. G. D. C. Samarasinghe and N. C. Pahalawaththa, "Damping of multimodal oscillations in power systems using variable structure control techniques," IEE Proc. Gen. Trans. and Distrib., Vol. 144, No. 3, 1997, pp. 323-331.

[5] Y.L. Abdel-Magid, M.A. Abido, S. Al-Baiyat and A. H. Mantawy, "Simultaneous Stabilization of Multimachine Power Systems via Genetic Algorithms," IEEE Trans. on Power Sys., Vol. 14, No. 4, November 1999, pp. 1428-1439.

[6] M.A. Abido and Y.L. Abdel-Magid, "Radial basis function network based power system stabilizers for multimachine power systems," Intl. Conf. Neural Networks, Vol. 2 , 9-12 June 1997, pp. 622 - 626

[7] A. Nabavi-Niaki, M.R. Iravani, "Steady-state and dynamic models of unified power flow controller (UPFC) for power system studies," IEEE Trans. Power Systems, Vol. 11, No. 4, Nov. 1996, pp 1937-1943

[8] H.F. Wang, "Damping function of unified power flow controller," IEE Proc. Generation Transmission and Distribution, Vol. 146, No. 1, 1999, pp 81-87.

[9] W.G. Heffron, R.A. Phillips, "Effect of modern amplidyne voltage regulators on under-excited operation of large turbine generator," AIEE Trans.

Power Apparatus and Systems, Aug 1952, pp 692-697.
[10] Z. Huang, Y. Ni, C.M. Shen, F.F. Wu, S. Chen, B. Zhang, "Application of unified power flow controller in interconnected power systems-modeling, interface, control strategy, and case study," IEEE Trans. Power Systems, Vol. 15, No. 2, May 2000, pp 817 -824
[11] T.K. Mok, Y. Ni, F.F. Wu, "Design of fuzzy damping controller of UPFC through genetic algorithm," IEEE Power Engineering Society Summer Meeting, Vol 3, 16-20 July 2000, pp 1889 - 1894
[12] P.K. Dash, S. Mishra, G. Panda, "A radial basis function neural network controller for UPFC," IEEE Trans. Power Systems, Vol. 15, No. 4 , Nov. 2000, pp 1293 -1299
[13] M. Vilathgamuwa, X. Zhu, S.S. Choi, "A robust control method to improve the performance of a unified power flow controller," Electric Power System Research, 55, 2000, pp 103-111.
[14] B.C. Pal, "Robust damping of interarea oscillations with unified power flow controller," IEE Proc. Generation Transmission and Distribution, Vol. 149, No. 6, 2002, pp 733-738.
[15] J.C. Seo, S. Moon, J.K. Park, J.W. Choe, "Design of a robust UPFC controller for enhancing the small signal stability in the multi-machine power systems," IEEE Power Engineering Society Winter Meeting, 2001. Vol. 3, 28 Jan.-1 Feb. 2001, pp 1197 -1202
[16] A. M. A. Hamdan, "An investigation of the significance of singular value decomposition in power system dynamics," Int. Journal of Electrical Power and Energy Systems, 21, 1999, pp 417-424
[17] Y.L. Abdel-Magid, M.A. Abido, "Robust coordinated design of excitation and TCSC-based stabilizers using genetic algorithm," Electric Power System Research, 69, 2004, pp 129-141.
[18] J. Kennedy, R. Eberhart, "Particle swarm optimization," Proc. IEEE Intl. Conf. Neural Networks, 4, Nov/Dec 1995, pp 1942 –1948.
[19] R. Eberhart, J. Kennedy, "A new optimizer using particle swarm theory," Proc. the Sixth Intl. Symposium on Micro Machine and Human Science, 1995. MHS '95, 4-6 Oct 1995, pp 39 -4